1. Experiment part

1.1 Synthesis of VC/nitrogen-doped carbon matrix (VC@NCM)

In a typic preparation, 1.2 g of PAN, and 1.5 g of VOC_2O_4 are dissolved into 15 mL DMF with magnetically stirring at 70 °C overnight to yeid electrospun solution. Then, the electrospun solution is continuously electrospun into the Al foil collector with a 19G of needle, a working distance of 15 cm, a feed rate of 0.1 mL min^{-1} and an applied voltage of 17.5 kV under 45°C. The collected nanofibers are annealed at 280°C for 2 h (5°C min^{-1}) and subsequently 1100°C for 1 h (2°C min^{-1}) under Ar flow to obtain VC@NCM.

For fair comparison, carbon fibers (no VOC_2O_4 used, defined as NCM) is also prepared.

1.2 Materials Characterization

The morphology and microstructure of materials is characterized by field-emission scanning electron microscope (FESEM; ZEISS Gemini 500). Transmission electron microscope (TEM), high-resolution transmission electron microscope (HR-TEM) and energy dispersive spectrometer mapping (EDS mapping) images are recorded with JEM-2100 HR. X-ray diffraction (XRD) patterns was carried out with BRUKER D8 ADVANCE and X-ray photoelectron spectra (XPS) are obtained by Thermos SCIENTIFIC ESCALAB 250Xi.

1.3 Electrochemical measurements

2032-type coin cells are assembled with lithium metal as counter electrode and reference electrode, celgard 2500 as separator and 10/16 μL 0.5 M Li_2S_6 catholyte dropped on VC@NCM or NCM with a diameter of 8 mm (sulfur loading of 1.91/3.05 mg cm^{-2}). The liquid electrolyte consisted of 1 M bistrifluoromethanesulfonylimide (LiTFSI) in 1, 2-dimethoxyethane (DME) and 1, 3-dioxolane (DOL) with volume ratio of 1:1, with 0.2 M $LiNO_3$ additive. The ratio of electrolyte to S is 20 uL mg^{-1}. Galvanostatic charge-discharge (GCD) electrochemical performance is tested between 1.8 and 2.8 V versus Li/Li$^+$ at various current densities on a NEWARE battery testing

system. Cyclic voltammetry (CV) measurements are performed using VMP-biologic electrochemical workstation. Electrochemical impedance spectroscopy (EIS) tests is carried out in the frequency range of 100 kHz to 100 mHz with an AC voltage amplitude of 5 mV.

1.4 Computational method

In this study, the density functional theory (DFT) calculation was implemented in the Vienna Ab-Initio Simulation Package. The electron-ion interaction was described by projector augmented-wave (PAW) pseudopotentials. For the exchange and correlation functionals, the Perdew-Burke-Ernzerhof (PBE) version of the generalized gradient approximation (GGA) exchance-correlation was used. In the adsorbed structures, 15 Å of vacuum layer thickness was applied to avoid virtual interaction and obtain more accurate results. The energy cutoff of 400 eV was used for the wave functions expansion. Brillouin zone integration on the grid with 4×4×2 for geometry optimization. The energy and force converged to 1.0×10^{-5} eV atom^{-1} and 0.03 eV·Å^{-1} to achieve high accuracy.

Thus, the corrected adsorption energy of Li_2S_6 (ΔE_{ads}) is defined as:

$$\Delta E_{ads} = E_{VC/Li2S6} - E_{VC} - E_{Li2S6}$$

Where $E_{VC/Li2S6}$ is the total energy of VC (200) adsorbed with Li_2S_6, E_{VC} is the total energy of the VC (200), and the E_{Li2S6} is the total energy of Li_2S_6.

Table S1. Electrical conductivity of various metal carbide and nitrides.

Compound	Electrical resistivity (uΩ cm)	Electrical conductivity (S cm^{-1})
VC	60	1.6×10^4
V$_2$C	150	0.64×10^4
VC$_{0.88}$	69	1.4×10^4
TiC	100	1.0×10^4
ZrC	75	1.3×10^4
HfC	67	1.4×10^4
Cr$_3$C$_2$	75	1.3×10^4
VN	65	1.5×10^4
CrN	640	1.5×10^3
NbN	60	1.6×10^4
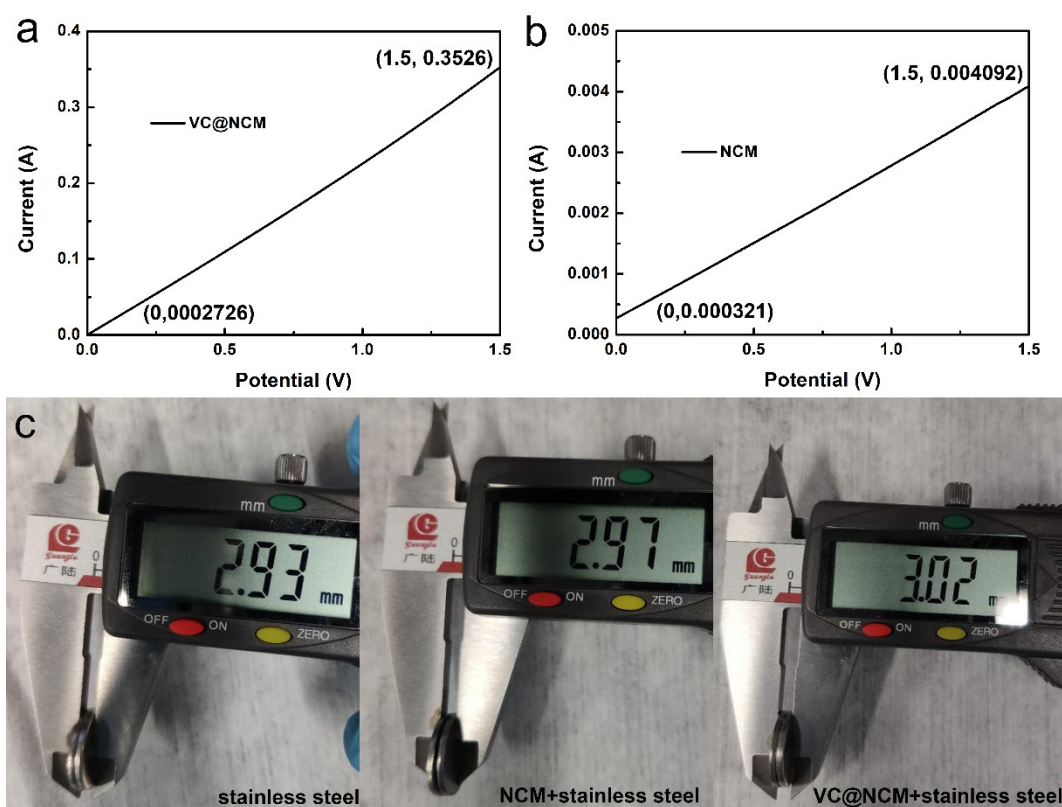
Figure S1. LSV curves of (a) VC@NCM and (b) NCM. (c) photos of thick measurement of VC@NCM and NCM disks.

Table S2. Electrical conductivity of VC@NCM and NCM.

Sample	Equation	R(Ω)	ρ (Ω·cm)	σ (S m^{-1})
VC@NCM	R=U/I=ρL/S	4.25	236.34	0.42
NCM	ρ=1/σ	366.57	45821.25	0.0021
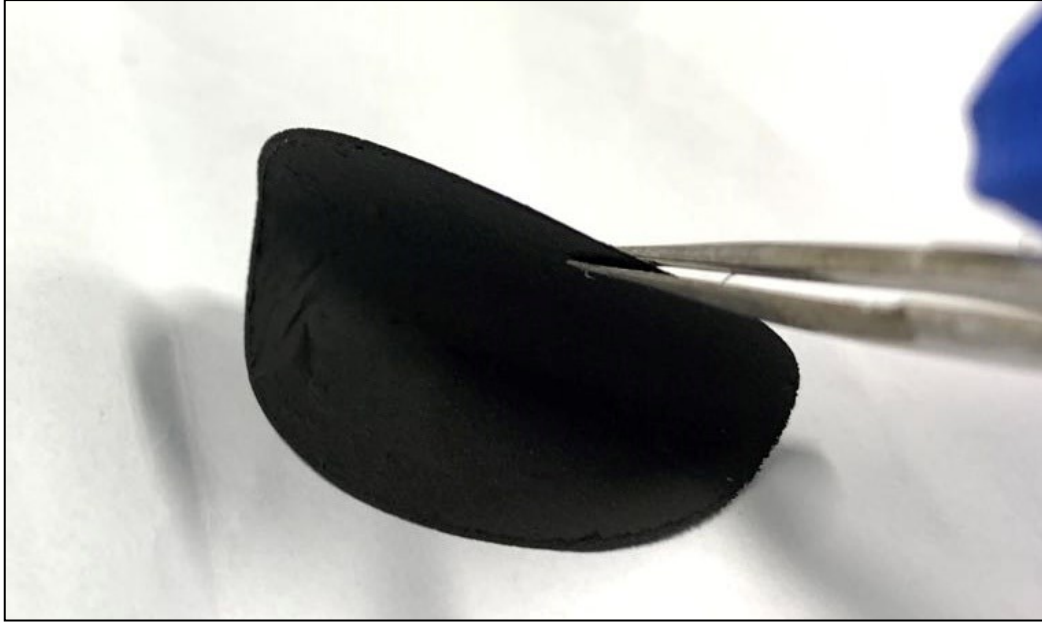
Figure S2. Photo of freestanding VC@NCM disk.
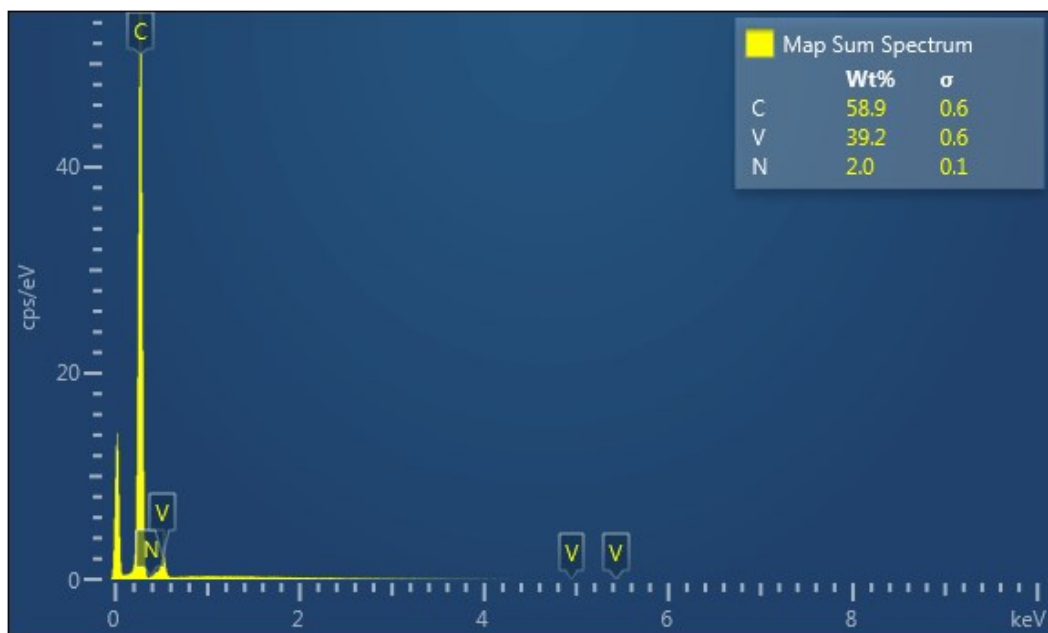
Figure S3. Element contents of C, N and V in VC@NCM.
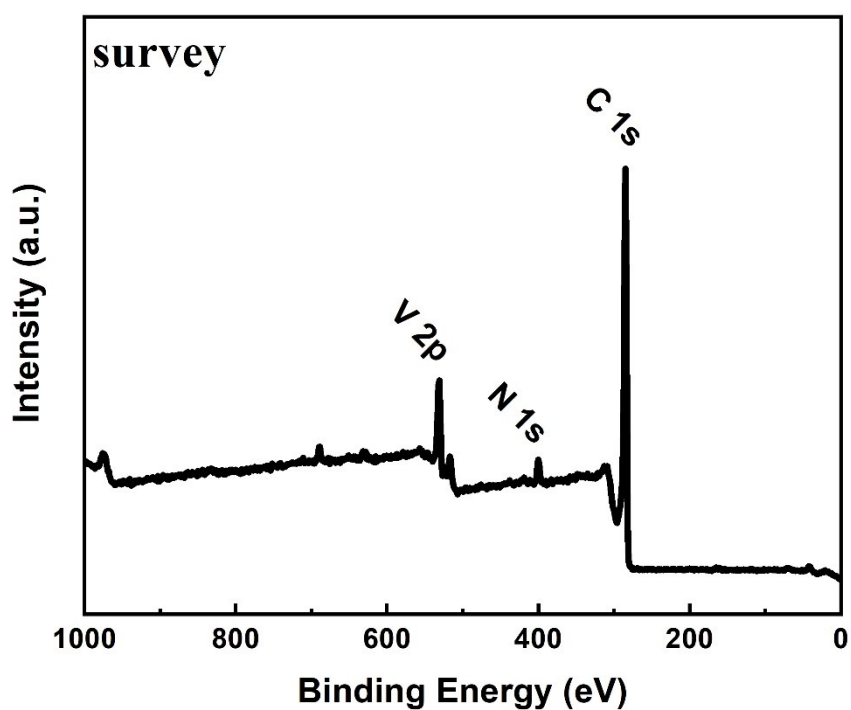
Figure S4. The XPS survey spectrum of VC@NCM.
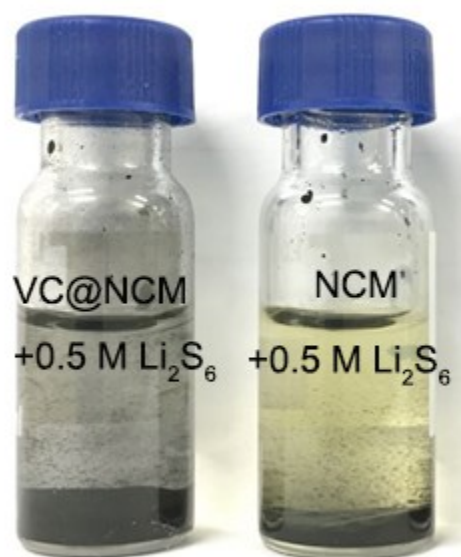
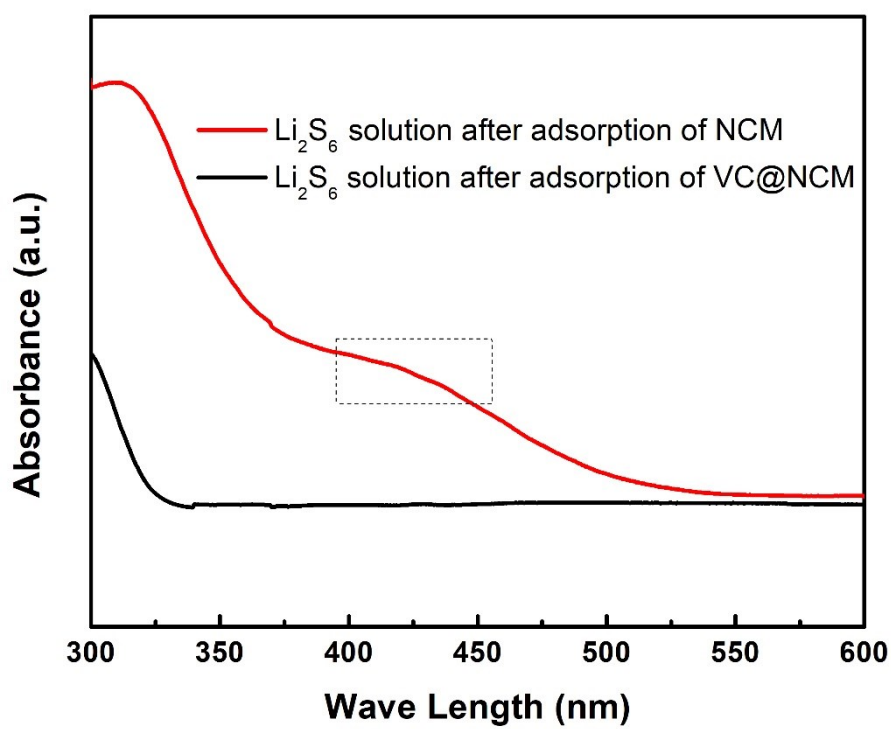Figure S5. Static adsorption of Li_2S_6 with VC@NCM and NCM after 24 h.

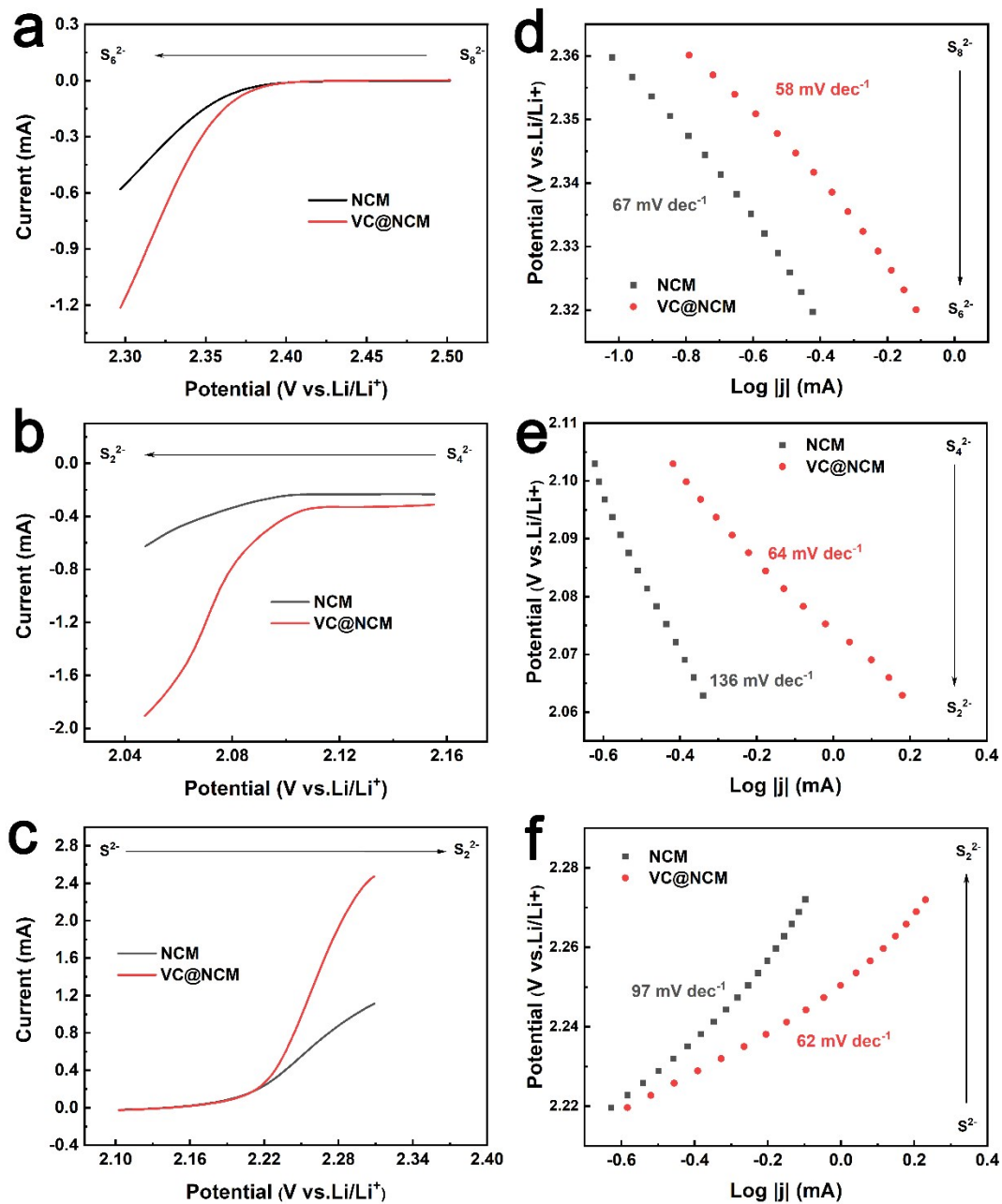Figure S6. UV–vis adsorption spectra of Li_2S_6 solution.

Figure S7. (a-c) The polarization curves of VC@NCM and NCM at different charge-discharge process and corresponding (d-f) Tafel plots.
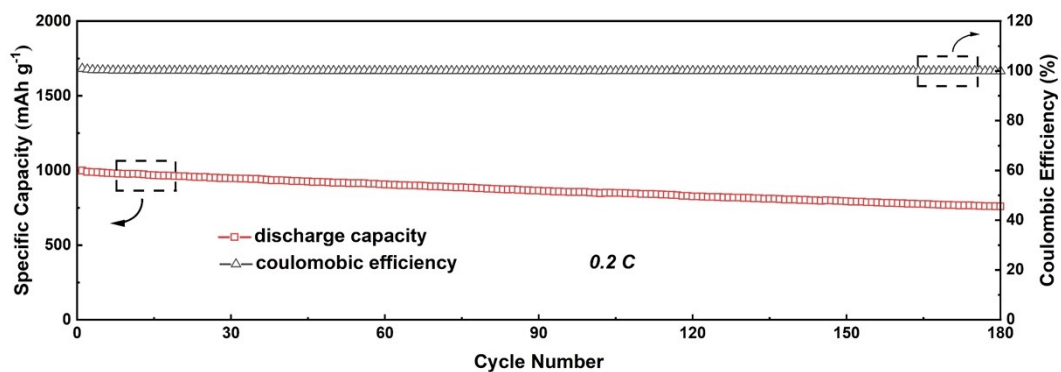
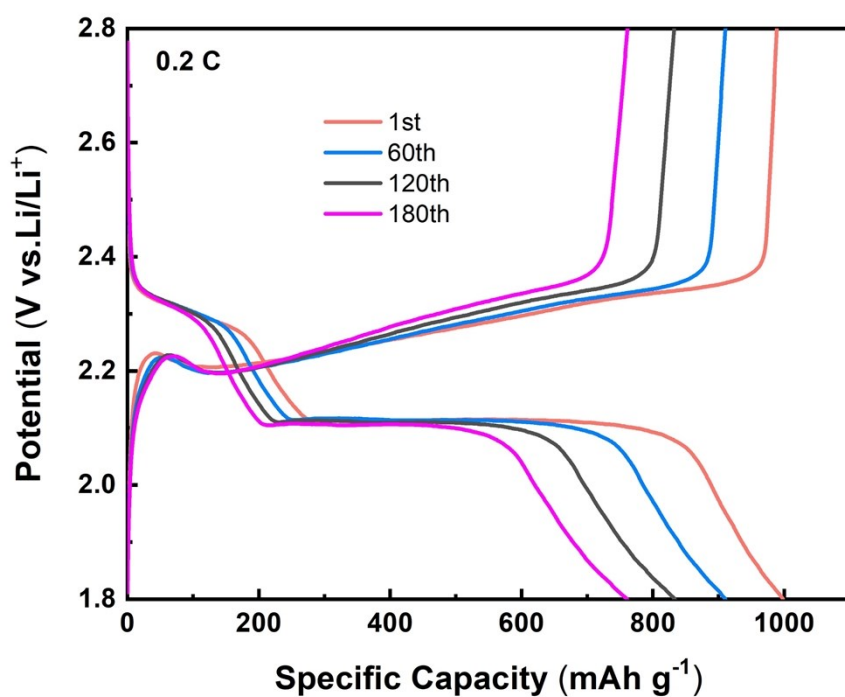Figure S8. Cycle performance of VC@NCM at 0.2C.
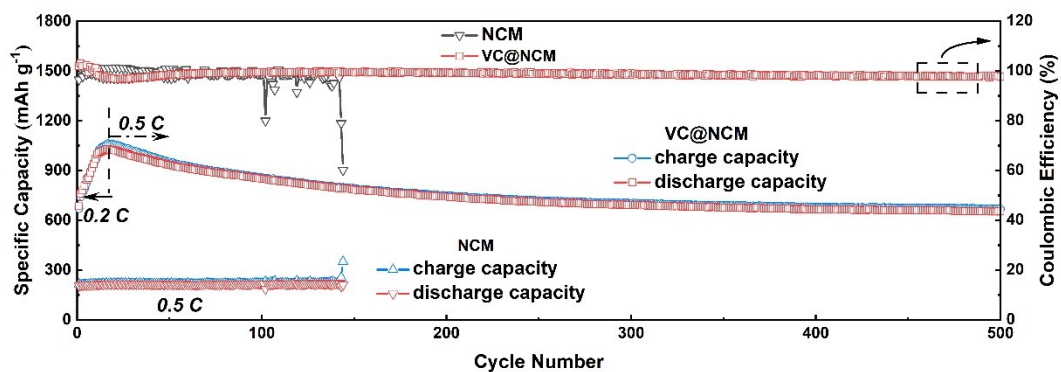

Figure S9. GCD curves of VC@NCM at 0.2 C.

Figure S10. Long-cycle performance of LSBs with VC@NCM or NCM for 500 cycles.
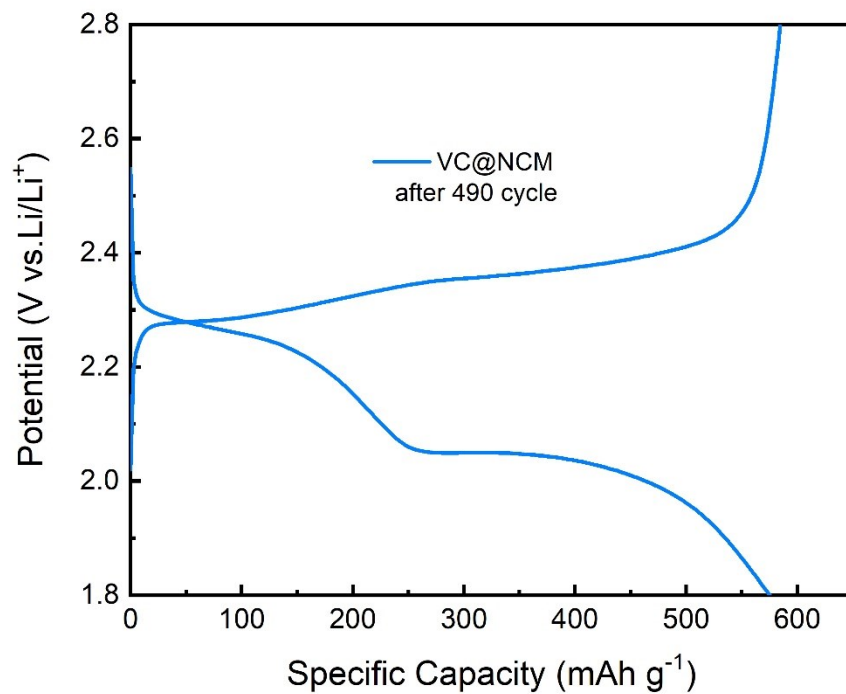

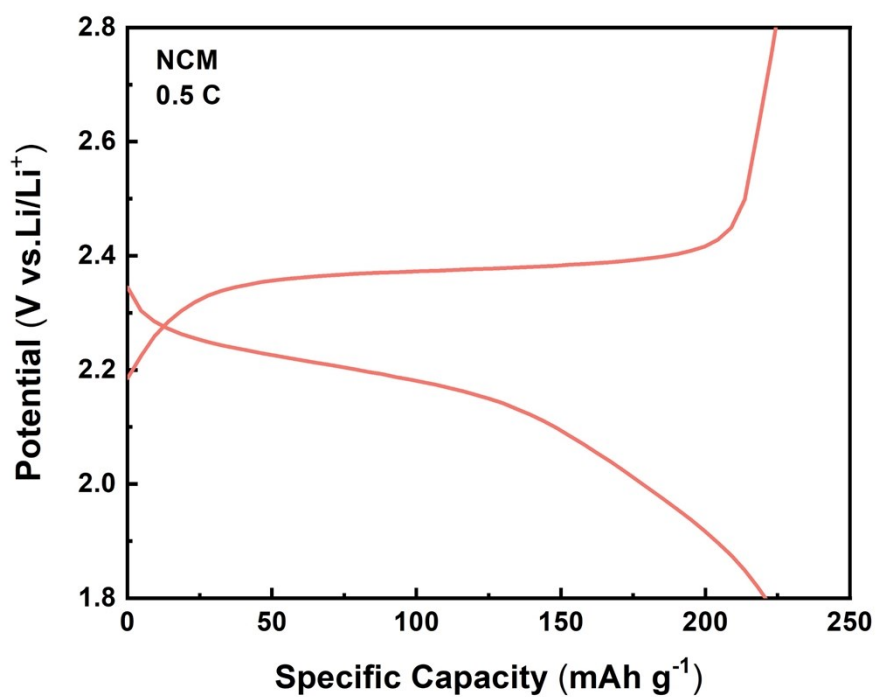Figure S11. GCD curves of VC@NCM at 0.5 C at 490$_{th}$ cycles.

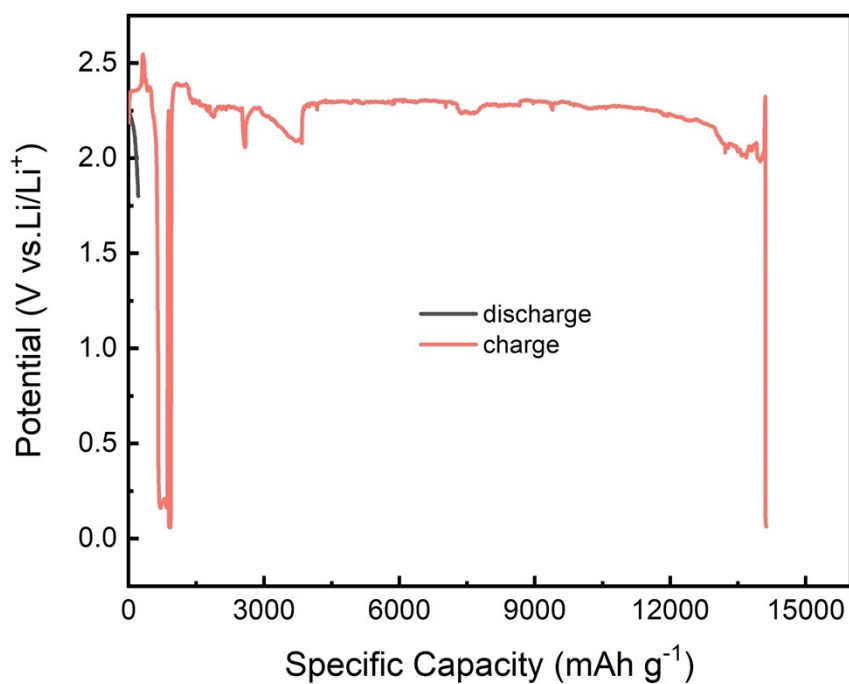Figure S12. GCD curves of NCM at 0.5 C at 140$_{th}$ cycles.

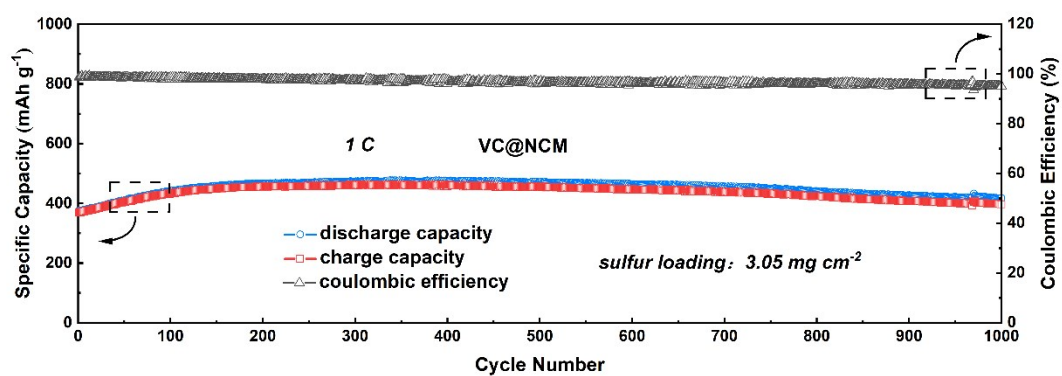Figure S13. Shuttle effect of NCM at 0.5 C after 140 cycles.

Figure S14. Long-cycle performance with VC@NCM at 1C with a higher sulfur loading of 3.05 mg cm^{-2}.

Table S3. Vanadium-based compound at rate of 1 C.

Compound	Sulfur loading (mg cm^{-2})	capacity after several cycles (mAh g^{-1})	capacity decay (per cycle)	reference

VC	**3.05**	**434 after 1000 cycles**	**0.01%**	**this work**
VO$_x$	1.8	374 after 600 cycles	0.025%	[1]
VO$_2$-VN	2.8	520 after 100 cycles	0.36%	[2]
V-N-C	1.0	392.6 after 500 cycles	0.087%	[3]
VN	2.8	636 after 200 cycles	0.19%	[4]

[1] Y. Zhang, X. Ge, Q. Kang, Z. Kong, Y. Wang, L. Zhan, Chem. Eng. J. 2020, 393, 124570.

[2] Y. Z. Song, W. Zhao, L. Kong, L. Zhang, X. Y. Zhu, Y. L. Shao, F. Ding, Q. Zhang, J. Y. Sun, Z. F. Liu, Energ. Environ. Sci. 2018, 11, 2620.

[3] Y. Fan, F. Ma, J. Liang, X. Chen, Z. Miao, S. Duan, L. Wang, T. Wang, J. Han, R. Cao, S. Jiao, Q. Li, Nanoscale 2020, 12, 584.

[4] X. Li, K. Ding, B. Gao, Q. Li, Y. Li, J. Fu, X. Zhang, P. K. Chu, K. Huo, Nano Energy 2017, 40, 655.